BMC Chemistry

RESEARCH

Open Access

Fabrication of an electrochemical sensor based on eggshell waste recycling for the voltammetric simultaneous detection of the antibiotics ofloxacin and ciprofloxacin

M. Khodari[1*], H. F. Assaf[1], Ahmed A. Shamroukh[1] and E. M. Rabie[1]

Abstract

In this work, an accurate, highly sensitive, and economical electrochemical sensor based on a carbon paste electrode modified by Ca_2CuO_3 nanostructure (Ca_2CuO_3 NS) was constructed using Eggshell waste recycling as a cheap source of calcium. The Ca_2CuO_3 NS was analyzed using FTIR, SEM, and XRD measurements. The synthesized nanomaterials utilized for the first time to enhance the electrocatalytic efficiency of carbon paste electrode (CPE) toward fluoroquinolones antibiotics ofloxacin (OFL) and ciprofloxacin (CIP), The drugs used to treat pneumonia caused by COVID-19. The synthesized Ca_2CuO_3 NS dramatically enhanced the anodic peak response of CPE toward both drugs compared to the unmodified one and other modified electrodes. The simultaneous detection of the two antibiotics was performed in the linear range of 0.09–1.0 µM for OFL and 0.05–0.8 µM for CIP with the LOD of 0.027 µM and 0.012 µM, respectively. The suggested method was applied successfully to determine OFL and CIP in real samples.

Keywords Electroanalytical methods, Chemical sensors, COVID-19, Nanostructure, Ciprofloxacin, Ofloxacin

Introduction

Fluoroquinolones (FQs), one of the most important classes of synthetic antibiotics, exhibit a broad-spectrum antibacterial effect, including Gram-negative and Gram-positive microorganisms [1, 2].Various FQs with various structural variations exhibit the same therapeutic efficacy because they depend on inhibiting bacterial DNA gyrase [3]. Because of their great activity, several FQs are frequently employed in hospitals, animal husbandry, and aquatic farming to prevent different diseases. Recently, many instances involving the use of various FQs in managing and treating COVID-19 have been reported worldwide [4]. Second-generation FQs of ofloxacin and ciprofloxacin are frequently prescribed to treat gonorrhoea, peritonitis, respiratory tract infections, osteomyelitis, gastrointestinal and soft tissue infections, and infections of the skin and other body tissues due to their high potency, low minimal inhibitory concentration, low toxicity, the long half-life, and high stability [1–5].

Structures of FQs are very similar; thus, it can be challenging to detect them simultaneously. However, several techniques, including spectroscopy [6, 7], chromatographic methods [8–10], and capillary electrophoresis [11], have been reported to identify FQs. These techniques can identify and separate FQs, but their general use is constrained by their complicated sample pretreatment procedures and pricey equipment. On the other hand, the electrochemical analysis approach has lately been used for FQs measurement due to its simplicity,

*Correspondence:
M. Khodari
khodari@svu.edu.eg
[1] Chemistry Department, Faculty of Science, South Valley University, Qena 83521, Egypt

© The Author(s) 2023. **Open Access** This article is licensed under a Creative Commons Attribution 4.0 International License, which permits use, sharing, adaptation, distribution and reproduction in any medium or format, as long as you give appropriate credit to the original author(s) and the source, provide a link to the Creative Commons licence, and indicate if changes were made. The images or other third party material in this article are included in the article's Creative Commons licence, unless indicated otherwise in a credit line to the material. If material is not included in the article's Creative Commons licence and your intended use is not permitted by statutory regulation or exceeds the permitted use, you will need to obtain permission directly from the copyright holder. To view a copy of this licence, visit http://creativecommons.org/licenses/by/4.0/. The Creative Commons Public Domain Dedication waiver (http://creativecommons.org/publicdomain/zero/1.0/) applies to the data made available in this article, unless otherwise stated in a credit line to the data.

speedy assay time, and affordable instrumentation [12, 13].

Carbon paste electrode (CPE) was frequently utilized as a working electrode in electroanalytical techniques because of its reusable surface, low cost, and simplicity of modification with a variety of materials, which allows the enhancement of the sensitivity and selectivity by increasing its activated surface area [14, 15]. To improve the sensing performance of CPE and to speed up the electron transfer rate for various redox systems, several metal oxide nanoparticles have recently been used to modify the surface of the CPE [16].

Recently, several nanocomposites have been utilized as a modifier to improve the performance of sensing electrodes, due to their superior chemical and physical properties such as morphology, electroactivity, and conductivity [17–19]. Cu-containing oxide materials such as Ca_2CuO_3 and $CaCu_2O_3$ are significant types of multimetal oxide materials that have received much attention owing to their unique features, including superconductivity and optical transparency. These systems stand out due to their more vital catalytic activity than pure components and larger surface area than pure oxides [20, 21].

Eggshells are a regular food waste that is generated in enormous quantities every day worldwide. The eggshell treatment is considered a cheap calcium source since $CaCO_3$ makes up a significant percentage of eggshell waste (more than 97%) [22, 23]. The manufacture of Ca_2CuO_3 NS in this study utilized eggshell waste as a natural, affordable, and biodegradable source of Ca. The mixed oxide produced was used to improve CPE's ability to simultaneously detect OFL and CIP antibiotics in real samples.

Here, a novel, accurate, highly sensitive, and economical electrochemical sensor based on eggshell waste recycling for the voltammetric detection of the antibiotics ofloxacin and ciprofloxacin was fabricated. Our strategy is based on eggshell waste recycling to extract Ca_2CuO_3 nanostructure, which in turn was used, for the first time, to modify CPE. The simultaneous detection of OFL and CIP antibiotics was achieved. The constructed sensor was successfully functionalized under optimal conditions for simultaneous sensing OFL and CIP in human serum and commercial pharmaceutical tablets with an acceptable recovery value (97.32% to 100.40%).

Experimental procedures

Materials

Pure OFL (≥ 99%) and CIP (≥ 98%) were purchased from Sigma-Aldrich (UK). Cupric chloride (powder, 99%) purchased from Merck (Germany). Graphite fine powder (98%) was purchased from LOBA Chemie company (India). Other reagents and chemicals of analytical grade were used in this investigation without further purification. Deionized water was used to prepare the utilized aqueous solutions. A refrigerator was used to store various stock solutions until usage in the lab. Daily prepared phosphate buffer solution (PBS) was applied as a supporting electrolyte.

Instruments

All electrochemical studies were carried out using Versa STAT4 and a three-electrode cell consisting of Ca_2CuO_3 NS/CPE, Ag/AgCl, and Pt wire as the working electrode, the reference electrode, and the counter electrode, respectively. A (Perkin Elmer) spectrometer was used for FT-IR analysis, and an XRD record was obtained at 25 °C employing (Brucker D8 Advance, Germany). SEM was used to examine the sample's surface morphology (JSM-5500 LV, Japan).

Synthesis of Ca_2CuO_3 powder

The coprecipitation method was utilized to prepare Ca_2CuO_3 powder, as described previously [24], with some modifications. In brief, the eggshell powder was prepared according to our previous work in the first step [22]. Then by considering that about 97% of eggshell waste consists of $CaCO_3$ [25], the appropriate weight of the resulting powder was dissolved in 100 ml HCl (1.0 M) to form $CaCl_2$ (1.0 M) solution. It was added to 100 ml of $CuCl_2$ (0.5 M), followed by the dropwise addition of NaOH (1 M) till pH = 12. The resulting powder was washed using deionized water, dried, and then calcinated at 900 °C for 3 h. Finally, the resulting powder was gathered and kept in a desiccator until characterization and electrocatalysis work.

Preparation of bare and modified carbon paste electrodes

The bare CPE (BCPE) was prepared as described previously elsewhere [12, 13]. Meanwhile, Ca_2CuO_3 NS/CPE was made by combining pure graphite, paraffin wax, and Ca_2CuO_3 NS by the percentage 60:25:15, respectively. The resulting mixture was heated to create a homogenous paste, and then the latter was inserted in a cylindrical plastic tube with an internal diameter of 3.91 mm. A copper wire was inserted and fixed in the paste to establish electrical contact with the external circuit. To activate the manufactured electrodes, a repetitive cyclic voltammetry between 0.0 and 1.0 V in a BR buffer solution (pH = 3.2) was applied till a fixed voltammogram was attained.

Preparation of real samples

Pharmaceutical samples

Ofloxacin® (400 mg) and Ciprofloxacin® (500 mg) were used as pharmaceutical samples for OFL and CIP, respectively. Five tablets of both samples were weighed

and powdered in a mortar individually. An appropriate amount of the resulting powder was dissolved in deionized water and filtered to remove inactive excipients. To attain the necessary drug concentration, the resultant solution was properly diluted with deionized water.

Human serum samples

Blood sample obtained from healthy volunteer was supplied by South valley University Hospital (The code of ethics of South Valley University was applied). To remove protein residues, 2.0 mL of methanol was added to 1.0 mL of the real sample that, was then diluted using PBS (0.1 M, pH 4.0) and subsequently centrifuged at 5000 rpm for 10 min. The supernatant was then saved for analysis. The quantification analysis was carried out employing the standard addition method.

Results and discussion

Characterization of Ca_2CuO_3 NS

To determine the chemical composition and purity of the synthesized Ca_2CuO_3 composite, EDX analytical measurement was used. Figure 1A shows the EDX pattern of Ca_2CuO_3; it is evident that the only components present are Ca, Cu, and O, indicating the high purity of the synthesized composite. The crystalline structure of the generated Ca_2CuO_3 NS was examined using XRD pattern analysis, shown in Fig. 1B. According to the standard COD (2002257 Ca_2CuO3), the obtained diffraction peaks were clearly attributed to the orthorhombic phase of Ca_2CuO_3 [20]. Using the Debye–Scherrer equation [26], the average crystalline size of the produced nanocomposite was calculated and found to be 42.3 nm. SEM was applied to characterize the morphological and visual characteristics of Ca_2CuO_3. Figure 1C demonstrates the morphology of Ca_2CuO_3, confirming

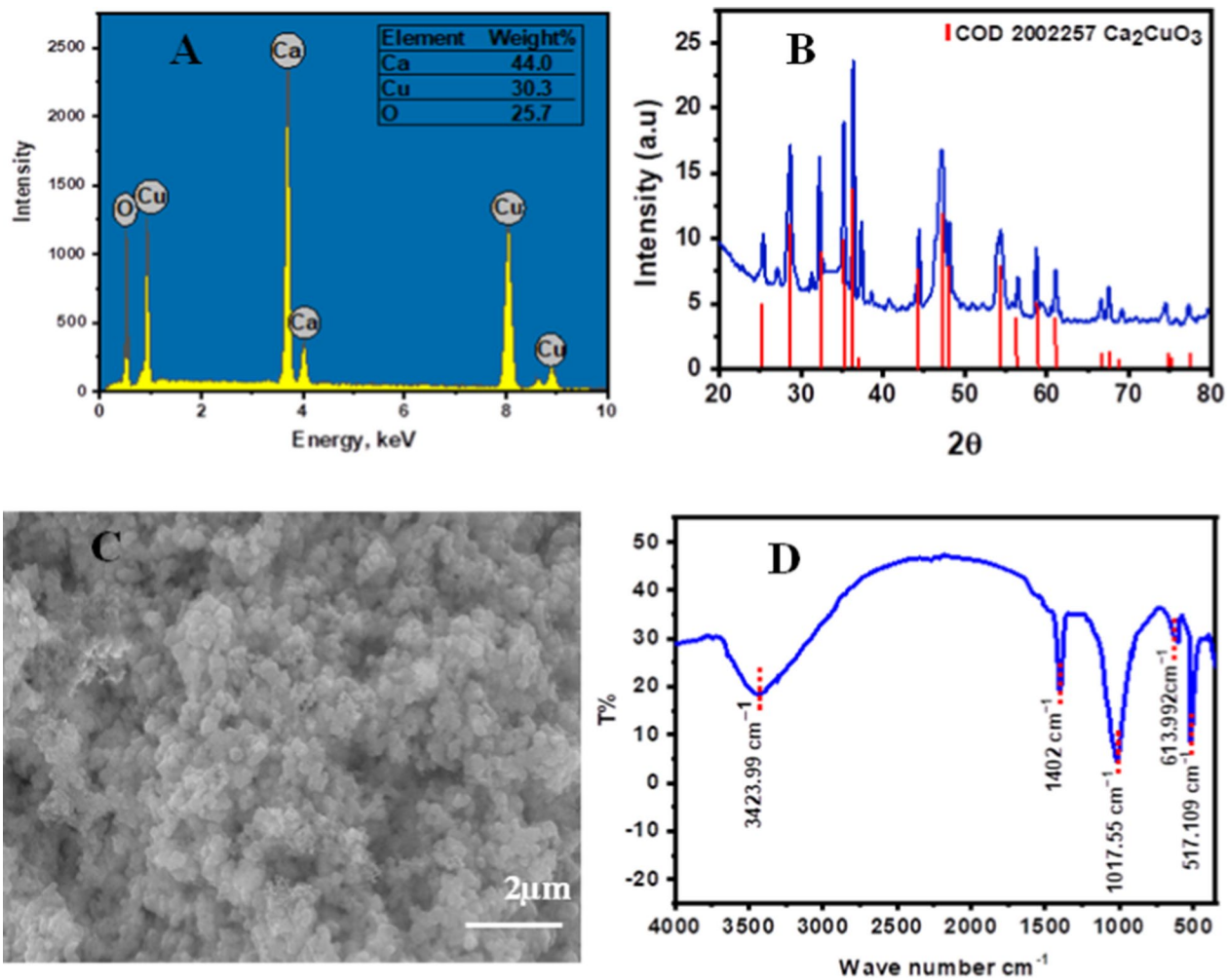

Fig. 1 EDX pattern of Ca_2CuO_3 (**A**), XRD patterns of Ca_2CuO_3 (**B**), SEM image of Ca_2CuO_3 (**C**), and FTIR spectrum of Ca_2CuO_3 (**D**)

the prepared composite's nanostructure and coral reef's structure. In order to examine the chemical structure of the produced spinal, FT-IR spectroscopy was utilized as well. As shown in Fig. 1D, the vibrations of Cu–O, Ca–O, and Ca–O–Cu have peaks at 517.109, 613.922, and 1017.55 cm^{-1}, respectively. The stretching vibration of unidentate carbonate caused by the adsorption of atmospheric CO_2 is shown by the absorption peak located at approximately 1402 cm^{-1} [27]. Additionally, a broad adsorption band located at about 3423.99 cm^{-1} is related to –OH vibration due to the absorbed water molecules when the prepared sample comes into contact with the atmospheric air [22, 27].

Electroactive surface area measurements

Cyclic voltammograms at BCPE and Ca_2CuO_3 NS/CPE in KCl (0.1 M) supporting electrolyte containing 1.0 mM of $[Fe(CN)_6]^{3-/4-}$ at a scan rate of 50 mV/s are shown in (Fig. 2). At both electrodes, $[Fe(CN)_6]^{3-/4-}$ displayed a reversible redox reaction with separation peak potentials (Ep) for BCPE and Ca_2CuO_3 NS/CPE of 0.512 V and 0.146 V, respectively. Additionally, compared to BCPE, the current signal at Ca_2CuO_3 NS/CPE is raised by 4.32 times. This finding demonstrates how Ca_2CuO_3 NS enhanced the electrochemical signal at the modified electrode and decreased the charge-transfer resistance, which promoted the electrochemical response of CPE. Thus, according to the obtained result, Ca_2CuO_3 NS/CPE has good electrocatalytic activity and can be applied for the appropriate analytical applications. The active surface area (A) for both applied electrodes was calculated using the Randles–Sevcik formula ($Ip = (26.9 \times 10^4)\ n^{1.5}\ AD_R^{0.5}\ \upsilon^{0.5}\ Co$) [14] and found to be 0.01 cm^2, and 0.067 cm^2 for BCPE and Ca_2CuO_3 NS/CPE, respectively. These results indicate that the Ca_2CuO_3 NS/CPE has a significantly higher electroactive surface area than BCPE.

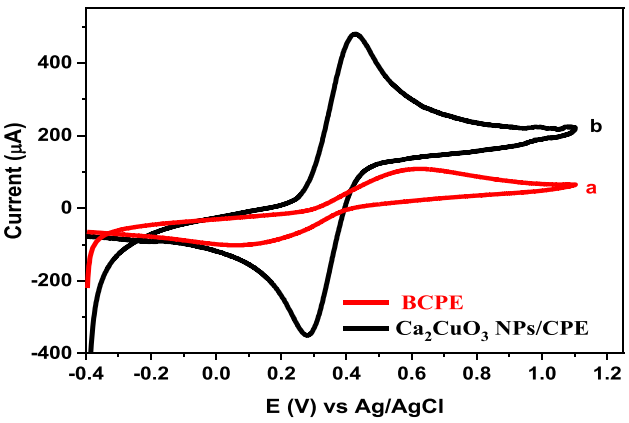

Fig. 2 Cyclic voltammograms of 1.0 mM $[Fe(CN)_6]^{3-/4-}$ in 0.1 M KCl and a scan rate of 50 mV/s at BCPE (**a**), and Ca_2CuO_3 NS/CPE (**b**)

Electrochemical behaviors of CIP and OFL at BCPE and Ca_2CuO_3 NS/CPE

As shown in Fig. 3, the electrochemical behaviors of OFL and CIP at BCPE and Ca_2CuO_3 NS/CPE were studied using the CV method in PBS (pH 4.0). The individual cyclic voltammograms for (1 µM) OFL and (0.5 µM) CIP at both electrodes were shown in Fig. 3A, B, as shown, both analytes exhibited an irreversible oxidation peak. Furthermore, it is obvious that the addition of Ca_2CuO_3 NS to CPE significantly increased the peak current signals, almost 4.7 times for OFL and 3.8 times for CIP compared to the anodic current signal at the surface of BCPE for the same concentrations. This enhancement may be attributable to the

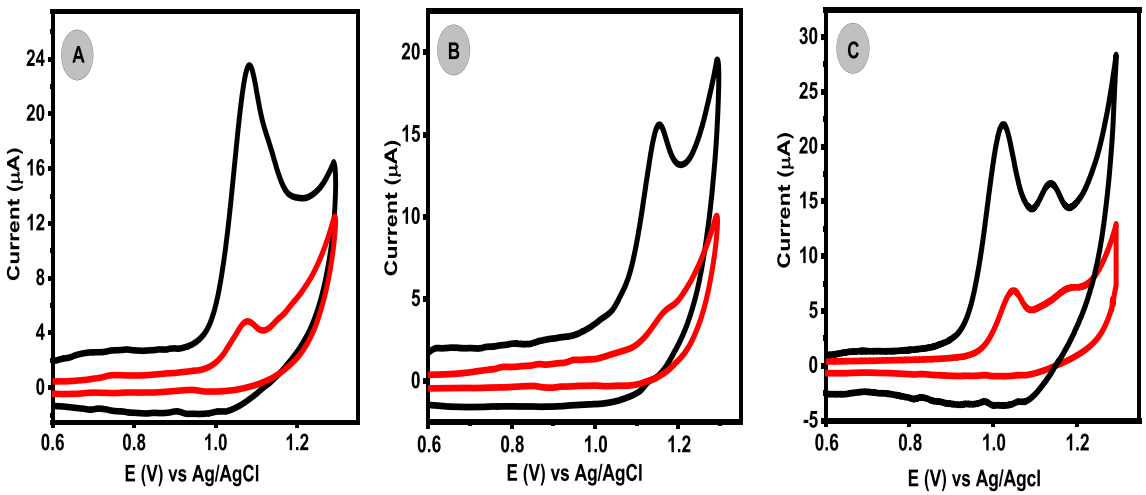

Fig. 3 Cyclic voltammograms of 1.0 µM OFL (**A**), 0.5 µM CIP (**B**), and the mixture of the two drugs (**C**) in the presence of (0.1 M, pH = 4) PBS scan rate of 50 mV/s. Redline for BCPE and black line for Ca_2CuO_3 NS/CPE

better adsorption capacity and strong catalytic activity of Ca_2CuO_3 NS, both are expected to improve the accumulation of the target analyte molecules at the modified electrode surface and expose more CPE active surface area [20, 28]. Obviously, the mixture of OFL and CIP drugs displayed two well-defined and sensitive anodic peaks with enhanced current response at the Ca_2CuO_3 NS/CPE, as shown in Fig. 3C. Additionally, the peak separation (ΔEp) value for both analytes was found to be 130 mV which is enough peak to peak separation that permitted the simultaneous determination of OFL and CIP at the Ca_2CuO_3 NS/CPE.

Effect of the pH

Linear sweep voltammetry (LSV) was utilized to investigate the impact of PBS pH value on the anodic response of 5 µM OFL and 3 µM CIP at the Ca_2CuO_3 NS/CPE surface Fig. 4. It was observed that the highest anodic current signals of OFL and CIP with maximum ΔEp resulted at pH 4. Thus, PBS of pH = 4 was used as the supporting electrolyte for further experiments. Additionally, the observation showed that by increasing the pH value from pH = 3 To pH = 7, the Ep shifted towards more negative values, illustrating the participation of protons in the oxidation process [29]. The linear relationship between Ep and pH for OFL and CIP are Ep(V) = 1.22–0.048 pH (r^2 = 0.990) and Ep(V) = 1.38–0.058 pH (r^2 = 0.988), respectively. The slopes for OFL and CIP, 0.048 and 0.058, respectively, show that the equivalent protons and electrons were involved in the electrochemical reaction [30]. These investigations follow the electrochemical reaction mechanisms of OFL and CIP as described in Scheme 1 [31, 32].

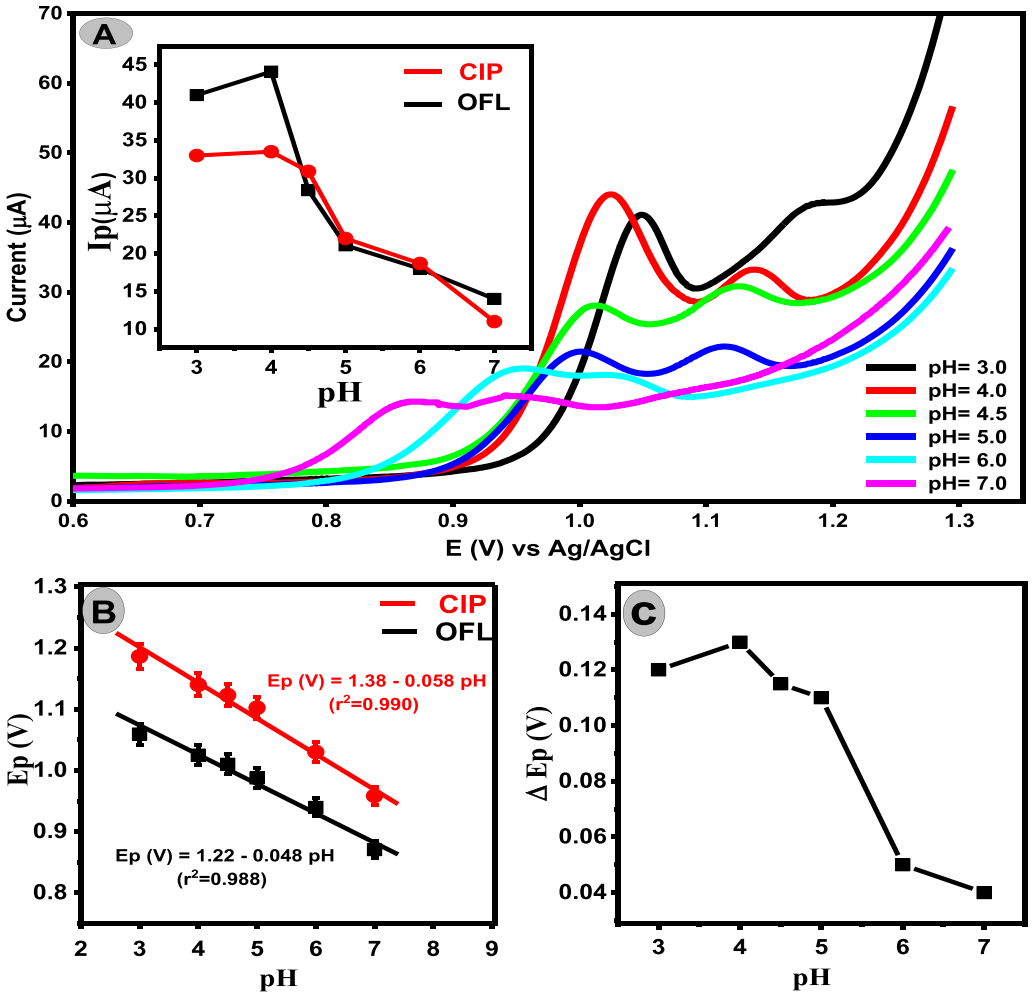

Fig. 4 **A** Linear sweep voltammograms of 5.0 µM OFL and 3.0 µM CIP mixture in PBS at different pH values and a scan rate of 50 mV/s on Ca_2CuO_3 NS/CPE. Insite relation between peak current of OFL (Black line) and CIP (Red line). **B** Dependence of Ep on pH for both drugs. **C** Dependence of potential peak separation ΔEp on pH

Effect of the scan rate

The effect of scan rate on the peak response. of 5.0 µM OFL and 5.0 µM CIP was investigated in PBS. Different scan rates were applied ranging from 30 to 500 mV in the presence of PBS and Ca_2CuO_3 NS/CPE as a working electrode. The recorded linear sweep voltmmograms are shown in Fig. 5. In which one can observe that on increasing the scan rate up to 500 mV/s, Ip of both drugs gradually increased, and Ep shifted positively. The results showed that Ip for both OFL and CIP is proportional to the square root of scan rate ($\upsilon^{1/2}$). Figure 3 inset demonstrates that the electrode reactions of OFL and CIP are diffusion controlled.

Meanwhile, on plotting log Ip versus log υ (Fig. 5B), a straight line with calculated slopes of 0.52 and 0.59 for OFL and CIP, respectively, the resulting slopes are close to 0.5, which indicates that the electrochemical oxidation of OFL and CIP at the Ca_2CuO_3 NS/CPE is diffusion-controlled [33]. Furthermore, Ep also showed a good linear relationship against the log υ for the two drugs (Fig. 5C).

According to Laviron's theory, as cited in [14], Ep/log(υ) can be described for an irreversible electrode process by the following equation at 25 °C.

$$\frac{\Delta Ep}{log\upsilon} = \frac{0.059}{\alpha n}, \tag{1}$$

where n represents the number of electron transfers in the rate-determining step and α symbolizes the charge transfer coefficient. According to Eq. (1), the αn was calculated to be 1.03 and 1.15 for OFL and CIP, respectively. Generally, α is granted to be 0.5, and n was found to be 2.06 for OFL and 2.3 for CIP, so the number of transfer electrons during the electrochemical oxidation for both analytes can be considered to equal 2. Due to the similarities in structure between OFL and CIP reported in the literature [31, 34], the probable oxidation reactions of OFL and CIP at Ca_2CuO_3 NS/CPE surface can describe as follows:

For OFL

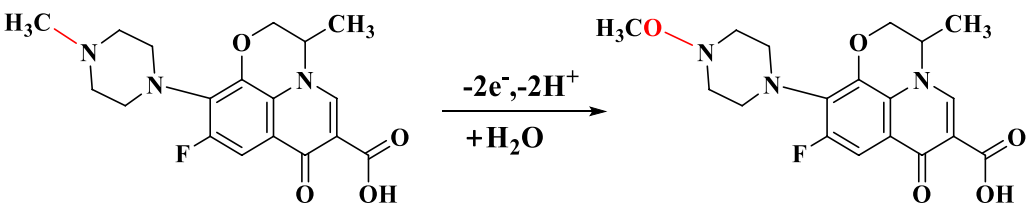

For CIP

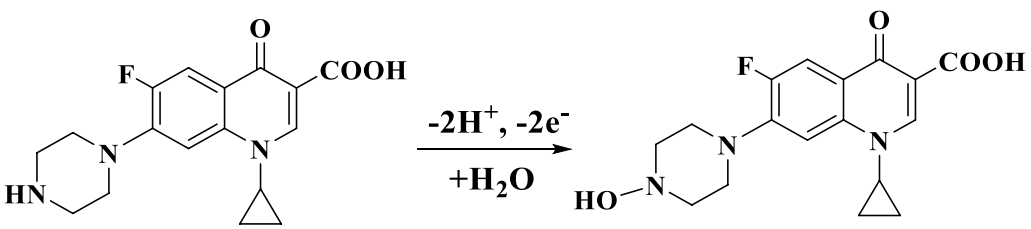

Chronoamperometric study

The chronoamperometric method was used to calculate the diffusion coefficient (D) values for the electrochemical oxidation of OFL and CIP at Ca_2CuO_3 NS/CPE surface by applying the Cottrell equation [35] Eq. (2)

$$Ip = nFAD^{1/2}C\pi^{-1/2}t^{-1/2}, \tag{2}$$

where A is the geometric surface area of the fabricated electrode (0.12 cm^2), C symbolizes the analyte concentration (mM), and t represents the time elapsed (s). (Fig. 6) demonstrates chronoamperograms of various concentrations of OFL (0.5–3.5 µM) and CIP (1.0–2.5 µM) at the potentials of 1.01 V and 1.14 V for OFL and CIP, respectively, in PBS (pH = 4.0). The relation between I and $t^{-1/2}$ resulted in straight lines for various concentrations of both analytes. The diffusion coefficient was found to be 2.40×10^{-7} cm^2/s and 4.03×10^{-6} for OFL and CIP, respectively.

Individual voltammetric determination of OFL and CIP

DPV was utilized to perform the individual electrochemical responses of OFL and CIP at Ca_2CuO_3 NS/CPE (the DPV parameters were optimized at a pulse height of 40 mV, pulse width of 0.005 s, step height of 15 mV, and step width of 0.01 s). As illustrated in Fig. 7, the anodic current signals increased linearly by increasing the concentration in the 0.01–7.5 µM range and 0.005–1.0 µM for OFL and CIP, respectively. LOD values were calculated to be 0.028 µM and 0.014 µM for OFL and CIP, respectively, according to S/N = 3. Additionally, LOQ values were estimated to be 0.094 µM and 0.046 µM, respectively according to S/N = 10. The outcomes demonstrated the significant sensitivity of

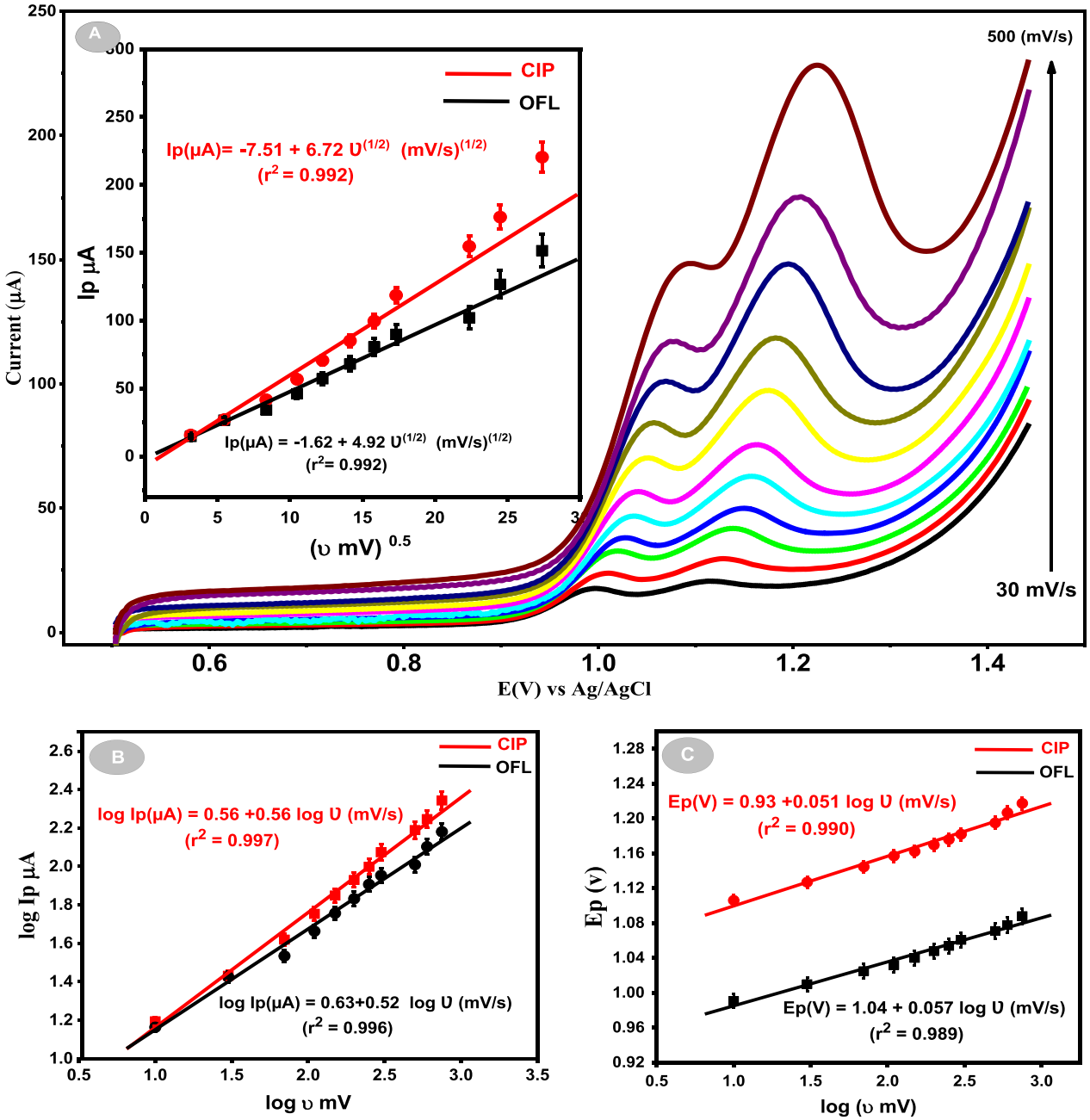

Fig. 5 **A** LSVs of 5 μM OFL and 3 μM CIP mixture in PBS (pH = 4) at various scan rates at Ca_2CuO_3 NS/CPE. Insite dependence of Ip (μA) on $\upsilon^{0.5}$ $(mV/s)^{0.5}$ for both OFL (Black line) and CIP (Red line). **B** Relation between log Ip (μA) and log υ (mV/s) for both drugs. **C** Relation between Ep (V) and log υ (mV/s)

the modified sensor toward the electrochemical oxidation of both drugs.

The proposed method is compared to previous methods used to determine OFL and CIP in Table 1. As illustrated in Table 1, different modifiers have been used to enhance the voltammetric performance of various sensors toward OFL and CIP detection. However, most of them are characterized by their relatively high cost. On the other hand, we developed an ecofriendly and cheap modified sensor in our work. Moreover, the developed method in this study showed lower LOD for OFL and CIP than most reported studies. As a result, due to the incontestable merits of the electrochemical method,

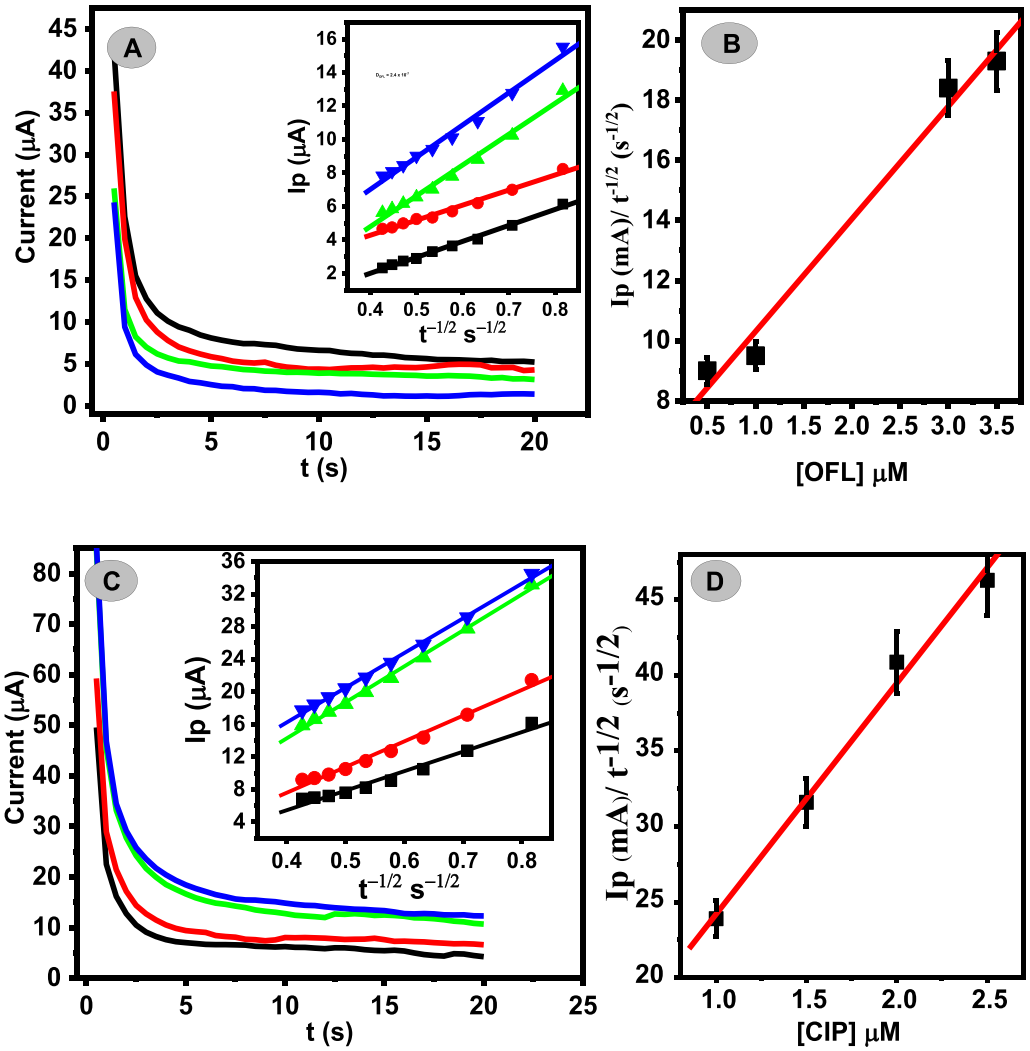

Fig. 6 **A** Chronoamperograms obtained at Ca_2CuO_3 NS/CPE in the presence of different OFL in PBS (0.1 M, pH = 4), inset dependence of OFL peak currents on the $t^{-1/2}$ derived from the chronoamperogram data, **B** plot of the corresponding slopes against OFL concentrations, **C** chronoamperograms obtained at Ca_2CuO_3 NS/CPE in the presence of different CIP concentrations in PBS (0.1 M, pH = 4), inset dependence of CIP peak currents on the $t^{-1/2}$ derived from the chronoamperogram data, **D** plot of the corresponding slopes against CIP concentrations

Ca_2CuO_3 NS/CPE will be a feasible voltammetric sensor for the quantification of OFL and CIP.

Simultaneous determination of OFL and CIP at Ca_2CuO_3 NS/CPE

To examine the applicability of Ca_2CuO_3 NS/CPE for the simultaneous detection of OFL and CIP in a mixture, DPV has been chosen to study the electrochemical oxidation responses of both drugs by the simultaneous change in the concentrations of OFL and CIP. As indicated in Fig. 8, Ip for both analytes increases linearly by increasing their concentrations in the range of 0.09–1 μM for OFL and 0.05–0.8 μM for CIP. LOD was calculated to be 0.027 μM and 0.012 μM for OFL and CIP, respectively, according to S/N = 3. These findings illustrate that Ca_2CuO_3 NS/CPE can be successfully applied for the simultaneous detection of OFL and CIP.

Interference, repeatability, and stability studies

The influences of some potential interference species of inorganic ions and organic compounds were studied under optimal conditions. The obtained results verified that about 150 folds of magnesium stearate, starch, lactose, poly (ethylene glycol), TiO_2, cellulose, talc, Zn^{2+}, Ca^{2+}, Na^+, K^+, Fe^{3+}, Cl^-, SO_4^{2-}, and about 100 times excess of ascorbic acid, uric acid, dopamine did not influence the electrochemical response of both drugs when the tolerance limit was considered as an ±5% error.

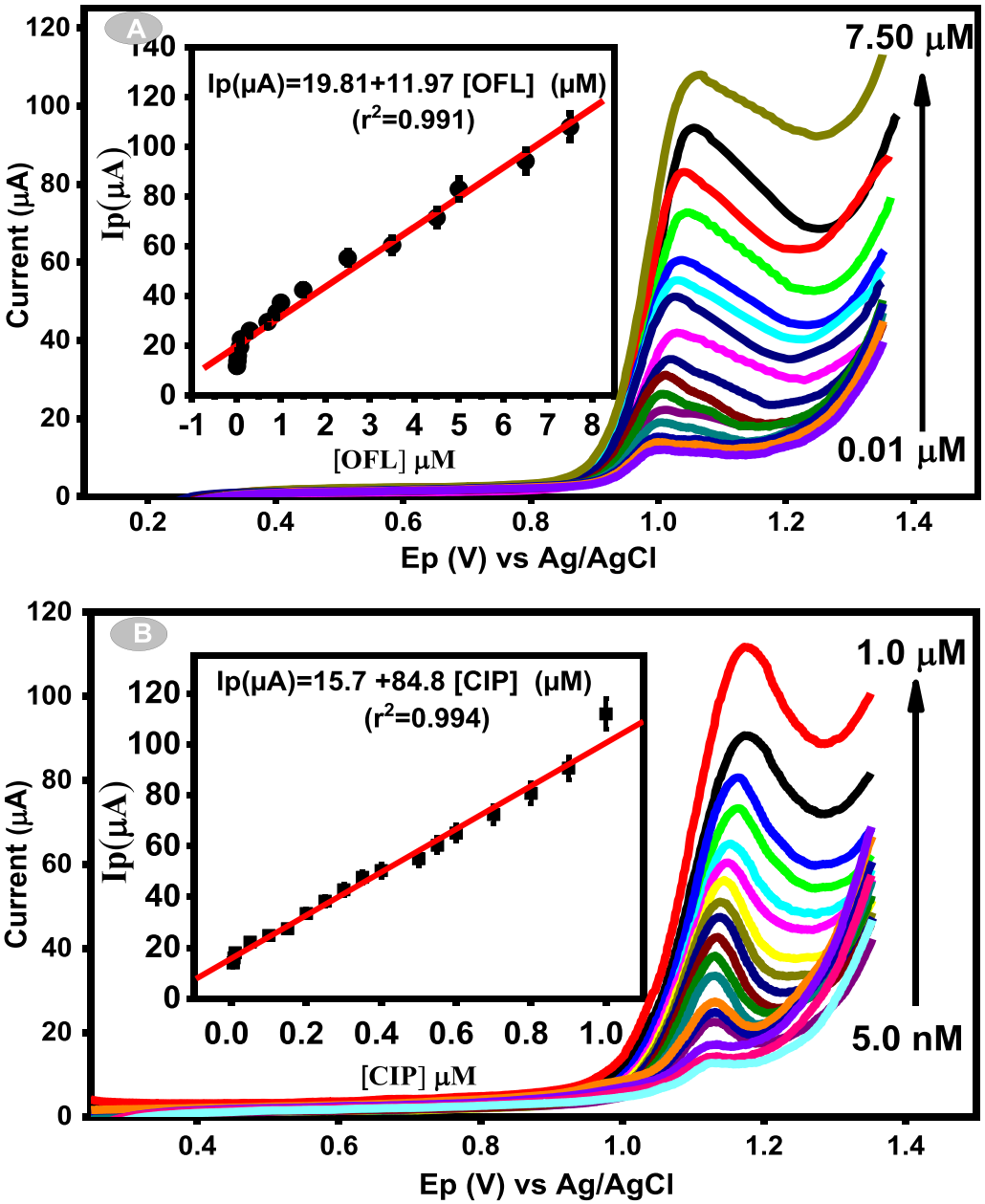

Fig. 7 **A**, **B** DPVs of individual detection of OFL (**A**) and CIP (**B**) at Ca_2CuO_3 NS/CPE in PBS (pH = 4). The inset in **A** and **B**: the corresponding calibration curve of OFL and CIP with different concentrations, respectively

Thus, it can be confirmed that Ca_2CuO_3 NS/CPE showed strong selectivity with no obvious interference effect on the detection of both fluoroquinolones.

The repeatability of the applied electrode was evaluated by measuring the same concentration using the same electrode for 6 successive measurements, and the calculated relative standard deviation (RSD) was found to be 3.9% for OFL and 2.43% for CIP, which indicated that the repeatability of Ca_2CuO_3 NS/CPE is satisfied.

The storage stability of Ca_2CuO_3 NS/CPE was also examined by the DPV response. The sensor was rinsed with PBS after each measurement and then stored at room temperature (~ 25 °C). A lowered voltametric response of the Ca_2CuO_3 NS/CPE of 3.9% to 5.1% was noted after 21 days for CIP and OFL, respectively, which demonstrates the high stability of Ca_2CuO_3 NS/CPE.

Table 1 Comparison of the linearity range and LOD for detecting OFL and CIP using various electrodes

Method	Working electrode	Analyte	Linear range [μM]	LOD [μM]	References
DPV	P-L CuO:Tb^{3+} NS/GCE	OFL	0.01–800.0	0.0019	[36]
DPV	TiN-gC/GCE	OFL	0.05–1.0	0.016	[37]
DPV	LGCE	OFL	25–200	0.75	[38]
DPV	Cu_2O/NG/Nafion/GCE	OFL	1.0–55	0.60	[39]
DPV	nAu@Ti_3C_2Tx/PABSA/GCE	OFL	0.05–500	0.037	[32]
DPV	Ca_2CuO_3 NS/CPE	OFL	0.01–7.5	0.028	Present Work
				0.027[a]	
DPV	Ch-AuMIP/GCE	CIP	1–100	0.21	[40]
DPV	MIP/rGO/GCE	CIP	10 -104	1.7	[41]
DPV	AuNPs/AC/GCE	CIP	0.005–0.025	0.002	[42]
SWAdAS	NiONPs-GO-CTS: EPH/GCE	CIP	0.040–0.97	0.006	[43]
DPV	Ca_2CuO_3 NS/CPE	CIP	0.005–1.0	0.014	Present work
				0.012[a]	

P-L CuO: Tb^{3+} NS, GCE, TiN-gC, LGCE, NG, PABSA, Ch-AuMIP, MIP/rGO, AuNPs/AC, and GO-CTS: EPH, mean peony-like dual-functional terbium doped copper oxide nanostructure, Glassy carbon electrode, Titanium nitrides nanoparticles/graphitic carbon, Laser modified Glassy carbon electrode, Poly-p-aminobenzene sulfonic acid, chitosan- gold molecular imprinted polymer, molecular imprinted polymer/reduced graphene oxide, Gold nanoparticles/Activated carbon, and graphene oxide-chitosan polysaccharide: EPH crosslinked agent, respectively

[a] Simultaneous detection

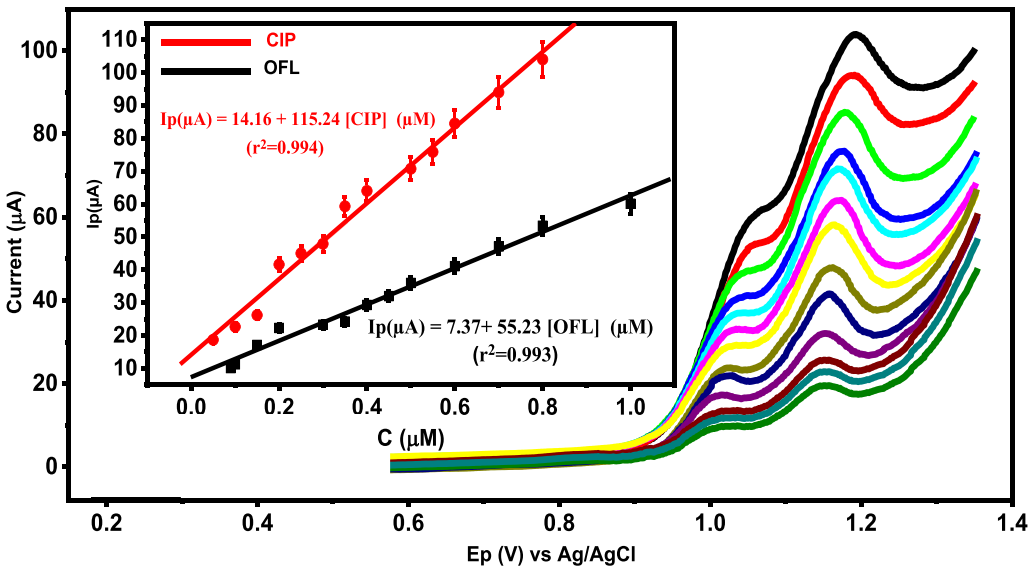

Fig. 8 DPVs of Ca_2CuO_3 NS/CPE at different concentrations of OFL and CIP. Insets the calibration curves for the simultaneous determination of OFL (black line) and CIP (red line)

Analytical applications

To confirm the applicability of the fabricated electrode in clinical applications, the Ca_2CuO_3 NS/CPE was utilized for detecting OFL and CIP concentrations in the pharmaceutical formulations Ofloxacin® (400 mg) and Ciprofloxacin® (500 mg), respectively. Additionally, Ca_2CuO_3 NS/CPE was utilized to detect OFL and CIP in human serum samples. As shown in Tables 2 and 3, recoveries between 97.32 and 100.40% were obtained, demonstrating a satisfactory level of accuracy for this method that may satisfy the needs of chemical analysis. Thus, the developed electrochemical sensor is applicable to determine OFL and CIP simultaneously.

Conclusions

This work achieved the conversion of eggshell waste into useful Ca_2CuO_3 NS with high catalytic activity. For the first time, the prepared Ca_2CuO_3 NS was utilized to

Table 2 DPV analysis of OFL and CIP in pharmaceutical samples at Ca_2CuO_3 NS/CPE

Tablet brand	Added (mg/20 mL)	Founded[a] (mg/20 mL)	RSD	[b]Recovery%
Ofloxacin® (500 mg)	20	19.65	3.78	98.25
	40	39.79	2.42	99.48
	60	58.39	1.25	97.32
Ciprofloxacin® (500 mg)	20	19.76	2.54	98.80
	40	40.06	1.79	100.15
	60	59.66	2.82	99.43

[a] Repeated at least three times

[b] Recovery = FoundedAdded × 100

Table 3 DPV analysis of OFL and CIP and human serum samples at Ca_2CuO_3 NS/CPE

Analyte	Added µM	Founded[a] µM	RSD	[b]Recovery (%)
OFL	0	0	–	–
	10	9.85	2.59	98.50
	20	19.59	2.41	97.95
	30	30.12	1.98	100.40
CIP	0	0	–	–
	5	4.95	3.36	99.00
	10	10.02	3.22	100.23
	15	14.75	2.18	98.33

[a] Repeated at least three times

[b] $Recovery = \frac{Founded}{Added} \times 100$

promote the electrocatalytic activity of CPE toward the simultaneous detection of two different fluoroquinolones antibiotics, OFL and CIP. The manufactured sensor was made with a special composition that is stable, repeatable, cheap, simple, sensitive, selective, and accurate towards both medicines. The individual detection of OFL and CIP can be performed in the range of 0.01–7.5 µM for OFL and 0.005–1.0 µM for CIP. LOD values were calculated as 0.028 µM and 0.014 µM for OFL and CIP, respectively. Additionally, the simultaneous detection of the two antibiotics was performed in the linear range of 0.09–1 µM for OFL and 0.05–0.8 µM for CIP with the LOD of 0.027 µM and 0.012 µM, respectively. Finally, Ca_2CuO_3 NS/CPE, with the aid of DPV offered an effective and inexpensive sensor for the successful simultaneous detection of OFL and CIP in pharmaceutical and human serum samples with an acceptable recovery value of (97.32% to 100.40%).

Abbreviations

Ca_2CuO_3 NS	Ca_2CuO_3 nanostructure
CPE	Carbon paste electrode
OFL	Ofloxacin
CIP	Ciprofloxacin
FQs	Fluoroquinolones
PBS	Phosphate buffer solution
CV	Cyclic voltammetry
LOD	Limit of detection
LOQ	Limit of quantification
LSV	Linear sweep voltammetry
DPV	Differential pulse voltammetry

Author contributions

MK and AAS have written the manuscript. EMR and HFA prepared the figures. All the authors reviewed the manuscript. The authors confirm the approval of the manuscript for submission. The authors confirm that the content of the manuscript has not been published or submitted for.

Funding

Open access funding provided by The Science, Technology & Innovation Funding Authority (STDF) in cooperation with The Egyptian Knowledge Bank (EKB).

Availability of data and materials

Data are available in request.

Declarations

Ethics approval and consent to participate

The authors confirm that all methods were carried out in accordance with relevant and guidelines and regulation or declaration of Helsinki. All the experimental protocol were approved by the ethical committee of south valley university. The SVU-code of ethics was used in this study. The author confirm that informed consent was obtained from subjects and or their legal guardians.

Consent for publication

The details of identifying images or other personal data or clinical participants are not applicable.

Competing interests

The authors declare that there is no competing interests.

Received: 29 May 2023 Accepted: 18 September 2023
Published online: 30 September 2023

References

1. Bilibio U, de Oliveira LH, Ferreira VS, Trindade MAG. Enhanced simultaneous electroanalytical determination of two fluoroquinolones by using surfactant media and a peak deconvolution procedure. Microchem J. 2014;116:47–54. https://doi.org/10.1016/j.microc.2014.04.009.
2. Zhu M, Li R, Lai M, Ye H, Long N, Ye J, Wang J. Copper nanoparticles incorporating a cationic surfactant-graphene modified carbon paste electrode for the simultaneous determination of gatifloxacin and pefloxacin. J Electroanal Chem. 2020;857: 113730. https://doi.org/10.1016/j.jelechem.2019.113730.
3. Zhang F, Gu S, Ding Y, Li L, Liu X. Simultaneous determination of ofloxacin and gatifloxacin on cysteic acid modified electrode in the presence of sodium dodecyl benzene sulfonate. Bioelectrochemistry. 2013;89:42–9. https://doi.org/10.1016/j.bioelechem.2012.08.008.
4. Karampela I, Dalamaga M. Could respiratory fluoroquinolones, levofloxacin and moxifloxacin, prove to be beneficial as an adjunct treatment in COVID-19? Arch Med Res. 2020;51:741–2. https://doi.org/10.1016/J.ARCMED.2020.06.004.
5. Oladipo AA, Oskouei SD, Review MG. Metal-organic framework-based nanomaterials as opto-electrochemical sensors for the detection of antibiotics and hormones: a review. Beilstein J Nanotechnol. 2023;14:52, 631–73. https://doi.org/10.3762/BJNANO.14.52.
6. Vosough M, Eshlaghi SN, Zadmard R. On the performance of multiway methods for simultaneous quantification of two fluoroquinolones in urine samples by fluorescence spectroscopy and second-order

calibration strategies. Spectrochim Acta A Mol Biomol Spectrosc. 2015;136:618–24. https://doi.org/10.1016/J.SAA.2014.09.075.
7. Osorio A, Toledo-Neira C, Bravo MA. Critical evaluation of third-order advantage with highly overlapped spectral signals. Determination of fluoroquinolones in fish-farming waters by fluorescence spectroscopy coupled to multivariate calibration. Talanta. 2019;204:438–45. https://doi.org/10.1016/J.TALANTA.2019.06.048.
8. Yu H, Tao Y, Chen D, Pan Y, Liu Z, Wang Y, Huang L, Dai M, Peng D, Wang X, Yuan Z. Simultaneous determination of fluoroquinolones in foods of animal origin by a high performance liquid chromatography and a liquid chromatography tandem mass spectrometry with accelerated solvent extraction. J Chromatogr B. 2012;885–886:150–9. https://doi.org/10.1016/J.JCHROMB.2011.12.016.
9. Meng Z, Shi Z, Liang S, Dong X, Li H, Sun H. Residues investigation of fluoroquinolones and sulphonamides and their metabolites in bovine milk by quantification and confirmation using ultra-performance liquid chromatography–tandem mass spectrometry. Food Chem. 2015;174:597–605. https://doi.org/10.1016/J.FOODCHEM.2014.11.067.
10. Alcaráz MR, Siano GG, Culzoni MJ, de la Peña AM, Goicoechea HC. Modeling four and three-way fast high-performance liquid chromatography with fluorescence detection data for quantitation of fluoroquinolones in water samples. Anal Chim Acta. 2014;809:37–46. https://doi.org/10.1016/J.ACA.2013.12.011.
11. Deng B, Li L, Shi A, Kang Y. Pharmacokinetics of pefloxacin mesylate in human urine using capillary electrophoresis electrochemiluminescence detection. J Chromatogr B. 2009;877:2585–8. https://doi.org/10.1016/J.JCHROMB.2009.06.021.
12. Rabie EM, Shamroukh AA, Khodari M. A novel electrochemical sensor based on modified carbon paste electrode with ZnO nanorods for the voltammetric determination of indole-3-acetic acid in plant seed extracts. Electroanalysis. 2022;34:883–91. https://doi.org/10.1002/elan.202100420.
13. Rabie E, Assaf HF, Elmaaref AA, Khodari M. Fabrication of a new electrochemical sensor based on carbon paste electrode modified by silica gel/MWCNTs for the voltammetric determination of salicylic acid in tomato. Egypt J Chem. 2019. https://doi.org/10.21608/ejchem.2019.17087.2048.
14. Tesfaye G, Negash N, Tessema M. Sensitive and selective determination of vitamin B2 in non-alcoholic beverage and milk samples at poly (glutamic acid)/zinc oxide nanoparticles modified carbon paste electrode. BMC Chem. 2022;16:1–17. https://doi.org/10.1186/S13065-022-00863-5/TABLES/3.
15. Nassar AM, Salah H, Hashem N, Khodari M, Assaf HF. Electrochemical sensor based on CuO nanoparticles fabricated from copper wire recycling-loaded carbon paste electrode for excellent detection of theophylline in pharmaceutical formulations. Electrocatalysis. 2022;13:154–64. https://doi.org/10.1007/S12678-021-00698-Z/TABLES/4.
16. George JM, Antony A, Mathew B. Metal oxide nanoparticles in electrochemical sensing and biosensing: a review. Microchim Acta. 2018;185:7, 1–26. https://doi.org/10.1007/S00604-018-2894-3.
17. Mehmandoust M, Soylak M, Erk N. Innovative molecularly imprinted electrochemical sensor for the nanomolar detection of tenofovir as an anti-HIV drug. Talanta. 2023;253: 123991. https://doi.org/10.1016/J.TALANTA.2022.123991.
18. Mehmandoust M, Çakar S, Özacar M, Erk N. The determination of timolol maleate using silver/tannic acid/titanium oxide nanocomposite as an electrochemical sensor in real samples. Electroanalysis. 2022;34:1150–62. https://doi.org/10.1002/ELAN.202100363.
19. Mehmandoust M, Uzcan F, Soylak M, Erk N. Dual-response electrochemical electrode for sensitive monitoring of topotecan and mitomycin as anticancer drugs in real samples. Chemosphere. 2022;291: 132809. https://doi.org/10.1016/J.CHEMOSPHERE.2021.132809.
20. Alikhanzadeh-Arani S, Salavati-Niasari M. Synthesize and characterization of Ca_2CuO_3 nanostructures via a modified sol-gel method assisted by hydrothermal process. J Clust Sci. 2012;23:1069–80. https://doi.org/10.1007/s10876-012-0499-2.
21. Salandari-Jolge N, Ensafi AA, Rezaei B. A novel three-dimensional network of $CuCr_2O_4$/CuO nanofibers for voltammetric determination of anticancer drug methotrexate. Anal Bioanal Chem. 2020;412:2443–53. https://doi.org/10.1007/S00216-020-02461-7/TABLES/1.
22. Assaf HF, Shamroukh AA, Rabie EM, Khodari M. Green synthesis of CaO nanoparticles conjugated with l-methionine polymer film to modify carbon paste electrode for the sensitive detection of levofloxacin antibiotic. Mater Chem Phys. 2023;294: 127054. https://doi.org/10.1016/J.MATCHEMPHYS.2022.127054.
23. Rabie EM, Shamroukh AA, Assaf HF, Khodari M. A novel sensor based on calcium oxide fabricated from eggshell waste conjugated with L-serine polymer film modified carbon paste electrode for sensitive detection of moxifloxacin in human serum and pharmaceutical constituents. Sens Actuators A Phys. 2023;356: 114351. https://doi.org/10.1016/J.SNA.2023.114351.
24. Veerapandi G, Lavanya N, Sekar C. Ca_2CuO_3 perovskite nanomaterial for electrochemical sensing of four different analytes in the xanthine derivatives family. Mater Chem Phys. 2023;295: 127076. https://doi.org/10.1016/j.matchemphys.2022.127076.
25. Jalu RG, Chamada TA, Kasirajan DR. Calcium oxide nanoparticles synthesis from hen eggshells for removal of lead (Pb(II)) from aqueous solution. Environ Chall. 2021;4: 100193. https://doi.org/10.1016/J.ENVC.2021.100193.
26. Vishwanath MS, Swamy BEK, Vishnumurthy KA. Electrochemical detection of bisphenol A in presence of catechol and hydroquinone at copper oxide modified carbon paste electrode. Mater Chem Phys. 2022;289: 126443. https://doi.org/10.1016/j.matchemphys.2022.126443.
27. Imtiaz A, Farrukh MA, Khaleeq-ur-rahman M, Adnan R. Micelle-assisted synthesis of Al_2O_3·CaO nanocatalyst: optical properties and their applications in photodegradation of 2,4,6-trinitrophenol. Sci World J. 2013;2013:1–11. https://doi.org/10.1155/2013/641420.
28. Mosaddegh E, Hassankhani A. Preparation, characterization, and catalytic activity of Ca_2CuO_3/$CaCu_2O_3$/CaO nanocomposite as a novel and bio-derived mixed metal oxide catalyst in the green synthesis of 2*H*-indazolo[2,1-b]phthalazine-triones. Catal Commun. 2015;71:65–9. https://doi.org/10.1016/j.catcom.2015.08.019.
29. Nabatian E, Mousavi M, Pournamdari M, Yoosefian M, Ahmadzadeh S. Voltammetric approach for pharmaceutical samples analysis; simultaneous quantitative determination of resorcinol and hydroquinone. BMC Chem. 2022;16:1–12. https://doi.org/10.1186/S13065-022-00905-Y/SCHEMES/1.
30. Fernandes IG, Chiorcea-Paquim AM, Oliveira-Brett AM. Calcium channel blocker lercanidipine electrochemistry using a carbon black–modified glassy carbon electrode. Anal Bioanal Chem. 2020;412:6381–9. https://doi.org/10.1007/S00216-020-02591-Y/FIGURES/6.
31. Wong A, Santos AM, Silva TA, Moraes FC, Fatibello-Filho O, Sotomayor MDPT. Sensitive and selective voltammetric determination of ciprofloxacin using screen-printed electrodes modified with carbon black and magnetic-molecularly imprinted polymer. Electroanalysis. 2023. https://doi.org/10.1002/elan.202200165.
32. Yang Z, Hu J, Zhang X, Yang H, Meng P, Zhao H, Sun Y. MXene-based composites as an electrochemical sensor for ultrasensitive determination of ofloxacin. Anal Bioanal Chem. 2023;415:157–66. https://doi.org/10.1007/s00216-022-04402-y.
33. Kassa A, Amare M. Poly(4-amino-3-hydroxynaphthalene-1-sulfonic acid) modified glassy carbon electrode for square wave voltammetric determination of amoxicillin in four tablet brands. BMC Chem. 2021;15:1–11. https://doi.org/10.1186/S13065-021-00739-0/TABLES/4.
34. Yang Z, Hu J, Zhang X, Yang H, Meng P, Zhao H, Sun Y. MXene-based composites as an electrochemical sensor for ultrasensitive determination of ofloxacin. Anal Bioanal Chem. 2022. https://doi.org/10.1007/S00216-022-04402-Y/FIGURES/4.
35. Nazari M, Asadollahzadeh H, Shahidi M, Rastakhiz N, Mohammadi SZ. Sensitive determination of hydroxylamine by using modified electrode by La_2O_3–Co_3O_4 nanocomposite and ionic liquid. Mater Chem Phys. 2022;286: 126209. https://doi.org/10.1016/J.MATCHEMPHYS.2022.126209.
36. Taherizadeh M, Jahani S, Moradalizadeh M, Foroughi MM. Synthesis of a dual-functional terbium doped copper oxide nanoflowers for high-efficiently electrochemical sensing of ofloxacin, pefloxacin and gatifloxacin. Talanta. 2023;255: 124216. https://doi.org/10.1016/j.talanta.2022.124216.
37. Wang C, Jing H, Li W, Long Y. One-step synthesis of TiN/C nanocomposites for the sensitive determination of ofloxacin. J Electrochem Soc. 2022;169: 087512. https://doi.org/10.1149/1945-7111/ac8770.
38. Feng L, Xue Q, Liu F, Cao Q, Feng J, Yang L, Zhang F. Voltammetric determination of ofloxacin by using a laser-modified carbon glassy electrode. Microchim Acta. 2020;187:86. https://doi.org/10.1007/s00604-019-4065-6.
39. Manjula N, Pulikkutty S, Chen T-W, Chen S-M, Liu X. Hexagon prism-shaped cerium ferrite embedded on GC electrode for electrochemical

detection of antibiotic drug ofloxacin in biological sample. Colloids Surf A Physicochem Eng Asp. 2021;627: 127129. https://doi.org/10.1016/j.colsurfa.2021.127129.
40. Surya SG, Khatoon S, Ait Lahcen A, Nguyen ATH, Dzantiev BB, Tarannum N, Salama KN. A chitosan gold nanoparticles molecularly imprinted polymer based ciprofloxacin sensor. RSC Adv. 2020;10:12823–32. https://doi.org/10.1039/D0RA01838D.
41. Bagheri H, Khoshsafar H, Amidi S, Hosseinzadeh Ardakani Y. Fabrication of an electrochemical sensor based on magnetic multi-walled carbon nanotubes for the determination of ciprofloxacin. Anal Methods. 2016;8:3383–90. https://doi.org/10.1039/C5AY03410H.
42. Gissawong N, Srijaranai S, Boonchiangma S, Uppachai P, Seehamart K, Jantrasee S, Moore E, Mukdasai S. An electrochemical sensor for voltammetric detection of ciprofloxacin using a glassy carbon electrode modified with activated carbon, gold nanoparticles and supramolecular solvent. Microchim Acta. 2021;188:208. https://doi.org/10.1007/s00604-021-04869-z.
43. Martin Santos A, Wong A, Araújo Almeida A, Fatibello-Filho O. Simultaneous determination of paracetamol and ciprofloxacin in biological fluid samples using a glassy carbon electrode modified with graphene oxide and nickel oxide nanoparticles. Talanta. 2017;174:610–8. https://doi.org/10.1016/j.talanta.2017.06.040.

Publisher's Note

Springer Nature remains neutral with regard to jurisdictional claims in published maps and institutional affiliations.

Ready to submit your research? Choose BMC and benefit from:

- fast, convenient online submission
- thorough peer review by experienced researchers in your field
- rapid publication on acceptance
- support for research data, including large and complex data types
- gold Open Access which fosters wider collaboration and increased citations
- maximum visibility for your research: over 100M website views per year

At BMC, research is always in progress.

Learn more biomedcentral.com/submissions